

# The effect of functionalized self-assembling peptide scaffolds on human aortic endothelial cell function

Elsa Genové<sup>a</sup>, Colette Shen<sup>b</sup>, Shuguang Zhang<sup>a,c</sup>, Carlos E. Semino<sup>a,c,\*</sup>

<sup>a</sup>Center for Biomedical Engineering, Massachusetts Institute of Technology, 77 Massachusetts Avenue, Cambridge, MA 02139, USA

<sup>b</sup>Harvard University, Cambridge, MA, 02138, USA

<sup>c</sup>Biotechnology Process Engineering Center, Massachusetts Institute of Technology, Cambridge, MA 02139, USA

Received 2 February 2004; accepted 10 August 2004

Available online 13 October 2004

## Abstract

A class of designed self-assembling peptide nanofiber scaffolds with more than 99% water content has been shown to be a good biological material for cell culture. Here, we report the functionalization of one of these peptide scaffolds, RAD16-I (AcN–RADARADARADARADA–CONH<sub>2</sub>), by direct solid phase synthesis extension at the amino terminal with three short-sequence motifs. These motifs are present in two major protein components of the basement membrane, laminin 1 (YIGSR, RYVVLPR) and collagen IV (TAGSCLRKFSTM). These motifs have been previously shown to promote specific biological activities including endothelial cell adhesion, spreading, and tubular formation. Therefore, the generic functionalized peptide developed was AcN–X–GG–RADARADARADARADA–CONH<sub>2</sub> with each motif represented by “X”. We show in this work that these tailor-made peptide scaffolds enhance the formation of confluent cell monolayers of human aortic endothelial cells (HAEC) in culture. Moreover, additional assays designed to evaluate endothelial cell function showed that HAEC monolayers obtained on these scaffolds not only maintained LDL uptake activity but also enhanced nitric oxide release and elevated laminin 1 and collagen IV deposition. These results suggest that this new scaffold provide a better physiological substrate for endothelial cell culture and suggest its further application for biomedical research, cancer biology and regenerative biology.

© 2004 Elsevier Ltd. All rights reserved.

**Keywords:** Self-assembly; Biomimetic material; Cell proliferation; Extracellular matrix; Endothelial monolayer

## 1. Introduction

We previously reported a self-assembling peptide nanofiber scaffold [1] that provides a good support material for cell culture [2]. However, self-assembling peptides can be modified with known functional peptide motifs from proteins of the basement membrane to promote specific cellular responses in similar way as other investigators have previously modified polymers

and biopolymers [3–8]. The basement membrane is a three-dimensional network composed mainly of laminins and collagens [9–12]. The basement membrane is not only important as a structural component, supporting cell attachment and providing boundaries between tissues and organs, but it also gives to the cells an instructive microenvironment that modulates their function. For instance, it is well established that the maintenance and function of endothelial cells are critically influenced by their interaction with the basement membrane [4,13–20]. Short sequences present in basement membrane proteins have been identified to participate in series of important biological functions, including cell migration and morphogenesis [4,13–20]. Laminin 1 is a heteroprotein that is formed by three

\*Corresponding author. Center for Biomedical Engineering, Massachusetts Institute of Technology, 77 Massachusetts Avenue, Cambridge, MA 02139, USA. Tel.: +1-617-258-0249; fax: +1-617-258-5239.

E-mail addresses: [shuguang@mit.edu](mailto:shuguang@mit.edu) (S. Zhang), [semino@mit.edu](mailto:semino@mit.edu) (C.E. Semino).

different polypeptide subunits,  $\alpha 1$ ,  $\beta 1$ , and  $\gamma 1$ , which assemble into a cross-like structure and that interacts as a connector or bridge between the cells and the extracellular matrix through several integrin and non-integrin receptors [11]. Two sequences present in the laminin-1  $\beta 1$  chain, YIGSR and RYVVLPR, have been shown to promote cell adhesion, cell migration, and endothelial cell tubular formation [3–6].

Type IV collagen, the other major component of the basement membrane, forms a network structure that involves its interaction with other components of the basement membrane, including laminin, nidogen, and heparan sulphate proteoglycan [21–23]. Collagen IV molecules are composed of two  $\alpha 1(\text{IV})$  chains and one  $\alpha 2(\text{IV})$  chains and can interact with cells indirectly through laminins by low affinity interactions [12,21] or by strong interactions mediated by nidogen, a glycoprotein of about 150 KDa, which bind tightly to laminin [22,23]. The peptide TAGSCLRKFSTM from the  $\alpha 1(\text{IV})$  chain of collagen IV was found to bind specifically to heparin in a dose-dependent manner [7,8] and to promote adhesion and spreading of bovine aortic endothelial cells [8]. Finally, in presence of heparin or chondroitin/dermatan sulphate glycosaminoglycan side chains, the binding of endothelial cells to the peptide TAGSCLRKFSTM was inhibited, suggesting that the peptide is a crucial domain involved in the determination of basement membrane ultra-structure, by connecting collagen IV with proteoglycans [11].

We selected self-assembling peptide nanofiber scaffolds to recreate a basement membrane analog. These peptides have a  $\beta$ -sheet structure and can self-assemble into a network of interweaving nanofibers of  $\sim 10$  nm diameter, forming hydrogel scaffolds with pores 5–200 nm in diameter and over 99% water content [1,2]. These peptide scaffolds have been shown to support attachment, growth, maintenance, and differentiation of a variety of mammalian cells [2,24–27]. For example, it supported differentiation of rat PC12 cells and functional synapse formation of rat primary hippocampal neurons [24], promoted bovine chondrocytes to develop cartilage constructs in vitro [25], and sustained differentiation of rat liver progenitor cells into functional hepatocyte-like cells [26]. In addition, the scaffold provides a new way of isolation of migrating hippocampal neural stem cells from organotypic cultures through a cell entrapment technique [27].

Previous investigators have studied the biological activity of the short peptide sequences Arg–Gly–Asp (RGD), which is present in fibronectin and other extracellular matrix proteins and is critical for cell adhesion, and Thy–Ile–Gly–Ser–Arg (YIGSR), which is present in laminin 1 and is important for cell function, after immobilizing them to glass surfaces and in two

synthetic polymers, polyethylene terephthalate (PET) and poly-(tetrafluoroethylene) (PTFE) [28]. The addition of these sequences has enhanced cell adhesion, cell spreading rate, and focal contact formation of human umbilical vein endothelial cells (HUVEC) cultured in these polymers that naturally possess very low-adhesive properties [28]. Similar results have been reported with endothelial cells after immobilizing the RGD peptide in synthetic polymers such as polyurethane (PEU) [29], polyvinyl alcohol (PVA) [30], and polyvinyl amine (PVAm) [31]. Recently, a class of self-assembling peptide exposing the bioactive peptide IKVAV from laminin has been described to form nanofiber scaffolds that can be used to select rapid differentiation of neural progenitor cells into neurons [32,33].

In this work, we report the functionalization of the peptide scaffold RAD16-I (AcN–RADARADARA–DARADA–CONH<sub>2</sub>) through direct solid phase synthesis extension at the amino terminal with three short-sequence motifs from two major proteins of the basement membrane, laminin 1 (YIGSR, RYVVLPR) and collagen IV (TAGSCLRKFSTM). We showed that these tailor-made scaffolds increased the formation of confluent cell monolayers with cobblestone phenotype of human aortic endothelial cells (HAEC) in culture with respect to non-modified peptide scaffolds. In parallel experiments consisting of culture HAEC on other substrate as controls including collagen I gels or Matrigel (natural basement membrane), similar monolayer formation was observed, suggesting that the functionalized peptide scaffolds may be considered like synthetic basement membrane analogs. Moreover, additional assays designed to evaluate endothelial cell function indicated that HAEC monolayers obtained on these scaffolds not only maintain LDL uptake activity but also enhanced nitric oxide release and elevated laminin 1 and collagen IV deposition. These results suggest that HAEC cultured on these new functionalized scaffolds enhanced the endothelial cell phenotype and promoted basement membrane deposition, which is a physiological prerequisite for successful culture and expansion of endothelial cells.

## 2. Materials and methods

### 2.1. Materials

All peptide sequences used in this work were obtained from SynPep Corporation ([www.synpep.com](http://www.synpep.com), Dublin, CA) and dissolved in deionized water at final concentration of 0.5% (5 mg/ml) and sonicated for 20 min (aquasonic, model 50 T, VWR, PA). Peptide hydrogel formation was developed on top of a cell chamber insert (10 mm diameter, 0.5 cm<sup>2</sup> area, pore size = 0.2  $\mu\text{m}$ , cat# 136935, Nalge Nunc International, IL), see below.

## 2.2. Circular dichroism (DC)

Circular dichroism (CD) spectra were gathered on an Aviv model 202 spectropolarimeter. Samples were prepared by diluting stock peptide solutions in water (0.5%) to a working concentration of 25  $\mu\text{M}$ . Samples were analysed at room temperature in a quartz cuvette with a path length of 0.3 cm and in the wavelength range 195–250 nm.

## 2.3. Atomic force microscopy (AFM)

Peptide from stock solutions (0.5%) were diluted to a working concentration of 0.01% (w/v). Atomic force microscopy (AFM) images were obtained with a Multi 75 silicon scanning probe (MPP-21100, Nanodevices Inc., CA) with a resonance frequency of 75 KHz, spring constant 3 N/m, tip curvature radius <10 nm and 225  $\mu\text{m}$  length. Images were obtained with a Multimode AFM microscope (Nanoscope IIIa, Digital Instruments, CA) operating in TappingMode. Typical scanning parameters were as follows: tapping frequency 75 KHz, RMS amplitude before engage 1–1.2 V, setpoint 0.7–0.9 V, integral and proportional gains of 0.2–0.6 and 0.4–1.0 respectively, and scan rate 1.51 Hz.

## 2.4. Rheometry

Rheological assays were performed on a 50 mm parallel plate ARES strain controlled rheometer (Rheometric Scientific, NJ). Samples were dissolved in deionized water at a final concentration of 2.9 mM and sonicated for 1 h the day prior to the analysis. A volume of 1 ml was loaded on the lower plate, and the upper plate was set to a gap size between 0.4 and 0.45 mm. Dynamic frequency sweep tests were performed in a range of frequencies from 100 to 0.1 rad/s. After the test, PBS was added around the lower plate in order to promote gelation. The peptide was allowed to gel for 10 min at room temperature before the test was performed once again. After a dynamic frequency sweep test, the behavior of samples over time was tested. A dynamic time sweep test was performed at 10 rad/s for 5 min.

## 2.5. Endothelial cell culture system

The scaffolds (0.5% w/v) were prepared at 100% peptide sequence for RAD16-I or blended with RAD16-I at a ratio of 9:1 (RAD16-I: peptide sequence; v/v) for the three other cases (YIG, RYV, and TAG, see Table 1). Each solution was sonicated for 30 min and filtered (0.2  $\mu\text{m}$ , Acrodysc filters, 4192, PALL, MI), loaded (100  $\mu\text{l}$ ) on top of a cell culture chamber insert (10 mm diameter, 136935, Nalge Nunc International, IL), and allowed to form a layer. Phosphate Buffer Saline (PBS)

Table 1  
Physicochemical and structural properties of peptide scaffolds used in this work

Name	Peptide sequence	Protein	Solubility in water 1% (w/v)	Gel formation (visual and rheometry)	Secondary structure (CD) <sup>a</sup>	Presence of nanofibers (AFM) <sup>b</sup>
RAD16-I	AcN-(RADA) <sub>4</sub> -CONH <sub>2</sub>	—	+	+	$\beta$ -sheet	+
YIG	AcN-YIGSR-GG-(RADA) <sub>4</sub> -CONH <sub>2</sub>	Laminin I	+	+	$\beta$ -sheet	+
RYV	AcN-RYVLPK-GG-(RADA) <sub>4</sub> -CONH <sub>2</sub>	Laminin I	+	+	$\beta$ -sheet	+
TAG	AcN-TAGSCLKFSM-GG-(RADA) <sub>4</sub> -CONH <sub>2</sub>	Collagen IV	+	+	$\beta$ -sheet	+

<sup>a</sup>Circular dichroism (CD).

<sup>b</sup>Atomic force microscopy (AFM).

was added at the bottom of the well to induce hydrogel formation. The system was incubated at room temperature for 30 min and PBS was exchanged by culture media twice and incubated for 1 h with endothelial cell growth media (EGM-2, Cambrex, MD) in a cell culture incubator at 37 °C with 5% CO<sub>2</sub>. Collagen I gel from rat tail (DB Biosciences, Bedford, MA) and Matrigel Matrix from EHS mouse tumor (DB Biosciences, Bedford, MA) were prepared following manufacture recommendations. Briefly, the solutions were loaded (100 µl) on top of same cell culture chamber insert and incubated in incubator at 37 °C with 5% CO<sub>2</sub> to allow gel formation. Meanwhile, HAEC (CC-2535, Cambrex, MD) from routine culture conditions (passage 5–6) were harvested and loaded on top of the preformed peptide scaffolds at a cell density of  $8 \times 10^4$  cells/cm<sup>2</sup> ( $\sim 6 \times 10^4$ /well) and cultured in the cell culture incubator at 37 °C with 5% CO<sub>2</sub>. Cell attachment assays were performed one hour after the initial cell loading. In this case, the covering media was removed, cells washed with PBS (without Ca<sup>2+</sup> and Mg<sup>2+</sup>) and incubated with Trypsin/EDTA (0.25%/0.1%, Gibco) for 30 min until most of the monolayer detached. Cells counting was performed on a hemacytometer after Trypan blue (T 9906, Sigma, MO) exclusion assay staining.

#### 2.6. NO release determination

Nitric oxide (NO) release was estimated by measuring nitrites (NO<sub>x</sub>) by the Griess method. Briefly, the media was replaced after the third day of culture by new media without fetal bovine serum (FBS) or ascorbic acid. The next day, the media was used to analyze NO release using a commercially available kit (482702, Calbiochem, CA) following the manufacturer instructions. Each condition was tested in triplicate.

#### 2.7. Competition assays with free soluble peptide sequences

HAEC were cultured as described above. For each scaffold, the respective soluble motif sequence and the non-respective sequence motifs were added independently to the media of HAEC cultures at a final concentration of 400 µg/ml. Half of the media was changed every other day. After the third day of culture, the media was removed, and fresh media without FBS or ascorbic acid containing 400 µg/ml of each soluble peptide motif was added. The next day, cell numbers were evaluated as described above. Each condition was tested in triplicate.

#### 2.7. PAGE-SDS and western blots

Harvested HAEC for each culture condition were counted and lysed with sample buffer (NP0007,

Invitrogen, CA) containing 2% (v/v) β-mercaptoethanol and a cocktail of protease inhibitors (1836153, Complete Mini, Roche, Penzberg, Germany) to avoid proteolysis. Cell lysates were developed on a 10% PAGE system in MOPS buffer (NP0301, NP0001 Invitrogen, CA), and proteins were transferred to PVDF membranes (LC2002, Invitrogen, CA) to perform western blots. Briefly, membranes were blocked with 2% BSA and 0.1% Triton-X 100 in PBS. Two primary antibodies were used: mouse monoclonal IgG<sub>1</sub> anti human laminin γ1 [laminin B2 chain] (1 µg/ml, B1920, Chemicon, CA) and mouse monoclonal IgG<sub>1</sub> anti human collagen IV [7S domain] (2 µg/ml, MAB3326, Chemicon, CA). A secondary antibody, goat polyclonal anti mouse IgG-HRP conjugated (1:5000 dilution, sc-2302, Santa Cruz Biotechnology, CA) was used for detection by chemiluminescent system (sc-2048, Santa Cruz Biotechnology, CA). Protein bands were visualized by exposure to an X-ray film (Biomax Film, Kodak, NY).

### 3. Results

#### 3.1. Design and synthesis of new tailor-made self-assembling RAD16-I peptides

The peptide scaffold RAD16-I was functionalized with laminin and collagen motifs in order to develop a basement membrane analog that enhances endothelial cell maintenance and function in vitro. We tailor-made the new peptide scaffolds by extending RAD16-I at the amino terminus through direct solid phase synthesis with three short peptide sequence motifs from two main components of the basement membrane, laminin 1 (YIGSR, RYVVLPR) and collagen IV (TAGSCLRFSTM). These modified peptide sequences obtained are listed in Table 1.

These peptides were soluble in water at concentration of 10 mg/ml (1% w/v) and formed hydrogels, suggesting their uses as scaffolds for cell culture. A molecular model representing the self-assembling peptide RAD16-I and the derived YIG is depicted in Fig. 1. The functionalized biological scaffolds offer several advantages including easy design and synthesis as well as the selection of an extensive repertoire of biological active motifs present in the extracellular matrix components.

#### 3.2. Physicochemical properties of the new functionalized peptides

In order to characterize the structural properties of the functionalized peptides, we studied several aspects, including secondary structure by CD, nanofiber formation by AFM, and scaffold viscosity properties by rheometry.

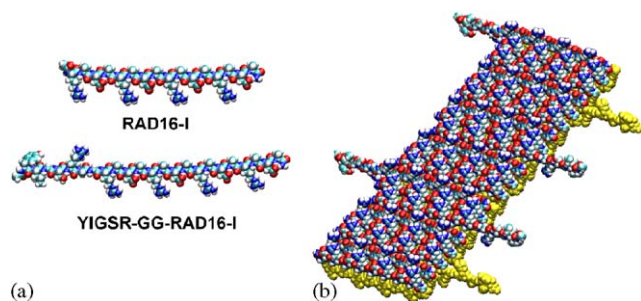


Fig. 1. Molecular models were built with CHARMM [34] and visualized using VMD [35]. (A) Model represents peptide RAD16-I (top) and peptide YIG (bottom) from Table 1. (B) Model representing a double  $\beta$ -sheet tape of a self-assembled peptide nanofiber of a mix composed of peptide RAD16-I: YIG (9:1). Note the sequences YIGSR extending out from the nanofiber tape.

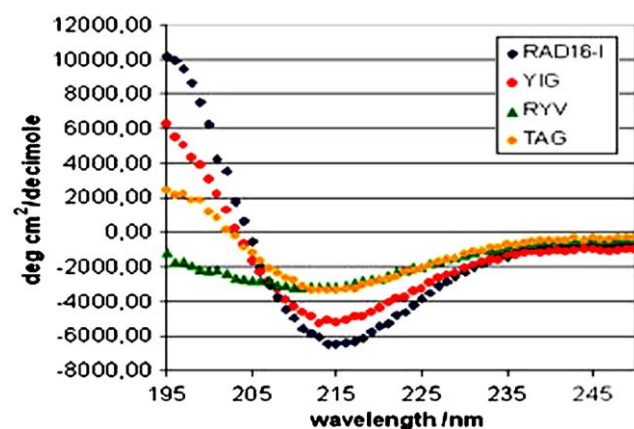


Fig. 2. Physicochemical characterization of peptides RAD16-I, YIG, RYV and TAG by CD (see materials and methods).

CD spectra were obtained for each peptide sequence to assess presence of  $\alpha$ -helices or  $\beta$ -sheets. A typical spectrum for  $\beta$ -sheet structures with a minimum mole residue ellipticity ( $\text{deg cm}^2/\text{decimole}$ ) at 216 nm and a maximum at 195 nm was observed for all peptides studied (Fig. 2). These functionalized peptides exhibited similar structural properties to the RAD16-I sequence (Fig. 2). The addition of the short peptide sequences reduced the  $\beta$ -sheet content, as shown by a decrease in the intensity of mole residue ellipticity at 216 nm (Fig. 2).

It has been previously reported that  $\beta$ -sheet structures of self-complementary peptides may be a requisite for self-assembly process into nanofibers [1,2]. We used TappingMode AFM to analyze the formation of nanofibers because this system allowed us to measure soft, fragile, and adhesive surfaces without damaging the samples. The presence of nanofibers in aqueous solutions was observed in all the four peptides present in Table 1 (Fig. 3). The AFM results not only confirmed the previous observation of hydrogel formation by

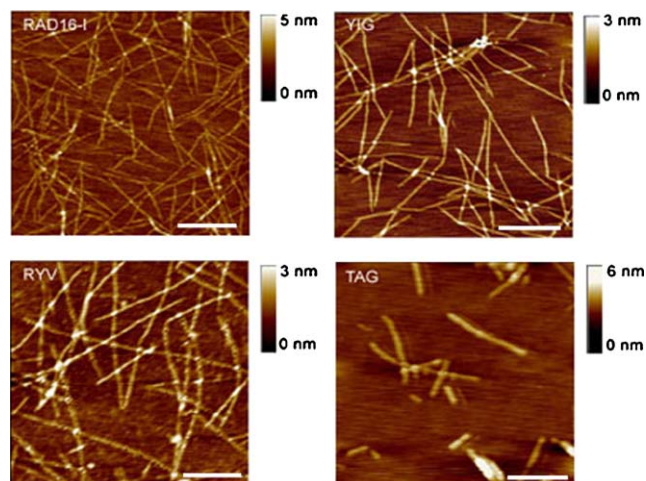


Fig. 3. Physicochemical characterization of peptides RAD16-I, YIG, RYV and TAG by AFM (see materials and methods).

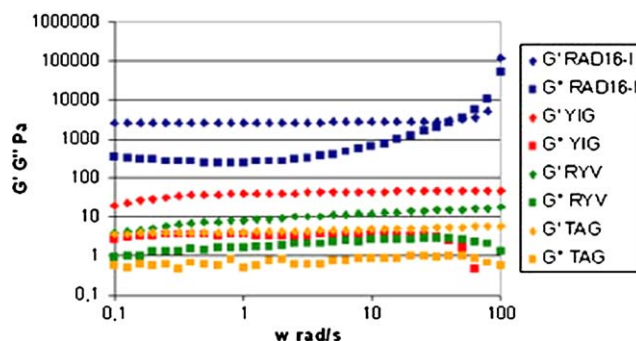


Fig. 4. Physicochemical characterization of peptides RAD16-I, YIG, RYV and TAG by Rheology: dynamic frequency sweep test for peptides scaffolds at fixed strain of 0.01.  $G'$  (Storage modulus) represents the elastic character of the material, and  $G''$  (Loss modulus) represents its viscous character (see materials and methods).

visual inspection, but also their potential use as scaffolds for tissue culture.

Rheological assays were performed to test the viscoelastic properties of each peptide in PBS buffer solution. In the case of RAD16-I,  $G'$  (storage modulus) is greater than  $G''$  (loss modulus), and both remain relatively constant with oscillatory frequency, indicative of a gel profile (Fig. 4). The storage modulus  $G'$  reaches  $2.5 \times 10^3$  Pa for this peptide (Fig. 4). The magnitude of  $G'$  is 100 times lower for the peptides YIG and RYV and 1000 times lower for the peptide TAG (Fig. 4). These results indicated that the addition of the additional motif interferes with the self-assembling process due to the possible distortion of the  $\beta$ -sheet configuration. This is consistent with the decrease in the intensity of mole residue ellipticity at 216 nm observed previous CD studies (Fig. 2). In addition, at a selected frequency of 10 rad/s applied 10 min after the initial measured (100 s, see Fig. 4) both moduli  $G'$  and  $G''$  remain constant with time (300 s), indicating that each gel has reached

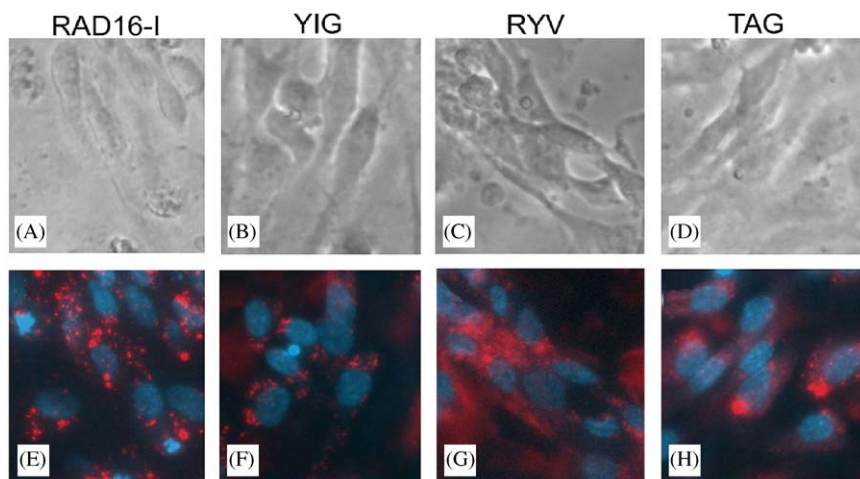


Fig. 5. Endothelial cell phenotype is maintained in HAEC cultured on peptide scaffolds RAD16-I, YIG, RYV and TAG (see Table 1). Phase contrast microscopy images of HAEC seeded on peptide scaffolds (A) RAD16-I; (B) YIG; (C) RYV; (D) TAG, and fluorescent staining with Di-Ac-LDL (red, LDL uptake) and DAPI nuclear staining (blue) for (E) RAD16-I; (F) YIG; (G) RYV; (H) TAG.

equilibrium with the buffer solution, maintaining stable rheological properties (not shown).

### 3.3. HAEC adhesion and monolayer formation on the functionalized peptide scaffolds

The main aim of the study was to obtain functionalized biomimetic scaffolds that can be used as synthetic basement membrane analogs to culture endothelial cells. We set up experiments in order to use these new scaffolds as instructive matrices to support growth and maintenance of HAEC by growing cells on the scaffold surface. Since aortic endothelial cells normally form monolayers that cover the internal surface of arteries, we tested whether the three modified peptide scaffolds would provide a better surface matrix than the RAD16-I by mimicking a basement membrane. In this experiment, we prepared four different scaffold surfaces, one composed of 100% RAD16-I and three composites consisting of 90% RAD16-I and 10% each of the modified peptides present in Table 1. Thus, the three final mixes in each case were named by their peptide names: YIG, RYV and TAG, respectively, with their surfaces tested having very similar mechanical properties (not shown). We seeded HAEC at subconfluent number (~50%) to allow good cell-material interaction. One hour after seeding, we counted unattached cells remaining in the supernatant media. We did not detect cells suspended in the media, indicating that the HAEC attachment to the surface was ~100% for all the scaffolds tested (not shown). This result suggests that the initial interaction of the cells with the material was not affected by the functionalization. In addition, cells growing on these four surfaces maintained basic endothelial cell phenotype, as evidenced by

LDL uptake (Fig. 5). Moreover, the capacity of endothelial monolayer formation was tested after culturing the cells for 3 days on the four peptide scaffold systems described above and two gel systems controls, collagen I gel and Matrigel (see materials and methods). Monolayer formation with typical confluent cobblestone phenotype was evidenced in all the gel systems tested with the exception of 100% RAD16-I gel where cells looked clustered with extended uncovered areas (Fig. 6). These results suggest that the modified peptide scaffold surfaces present similar properties as the natural materials used (collagen I gel and Matrigel) in terms of mimicking biological basement membranes.

### 3.4. HAEC growth on functionalized peptide scaffolds

In order to analyze the growth of HAEC on each scaffold surface, cells were seeded under subconfluent conditions (~50%) and after 3 days in culture cell number and viability were calculated for each condition. Interestingly, cell numbers increased about two-folds on the modified peptide scaffolds with respect to the RAD16-I control (Fig. 7B). Parallel cultures performed on collagen I gel and Matrigel promoted similar cell growth as observed for the modified peptide scaffolds (data not shown). This change in the growth accelerated the formation of a confluent monolayer with cobblestone phenotype on the modified surfaces (for reference see Fig. 6), suggesting that cells may sense and respond to the motif-modified material. To confirm this idea, competition assays with each free peptide motif were performed in order to specifically block the interaction between the cell surface and the modified material scaffold. In all cases, soluble peptides YIGSR (S.P.

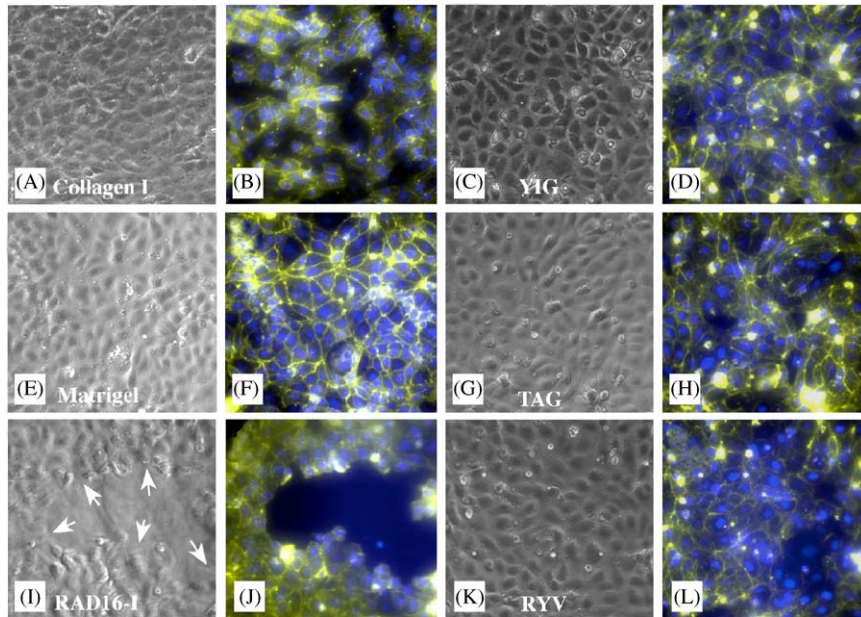


Fig. 6. Monolayer formation of HAEC cultured on different gel systems. Phase contrast microscopy images of HAEC cultured for 3 days on Collagen I gel (A), Matrigel (C), 100% peptide scaffold RAD16-I (E), blending 90% RAD16-I/10% (v/v) YIG (G), blending 90% RAD16-I/10% (v/v) TAG (I), blending 90% RAD16-I/10% (v/v) RYV (K). Fluorescent staining of the same optical layers with TRITC-Phalloidin and DAPI in order to detect actin fibers (yellow) and nucleus (blue), respectively, for A (B), C (D), E (F), G (H), I (J), K (L). Phase contrast and fluorescent images depict a typical cobblestone monolayer phenotype. White arrows in E indicate the borders of the non-confluent monolayer.

YIP), RYVVLPR (S.P. RYV), and TAGSCLRKFSTM (S.P. TAG) added to the culture media of their specific modified peptide scaffold reduced cell growth after 3 days in culture to similar levels as the RAD16-I (Fig. 7A and B). These results suggest that cells specifically recognize the functional sequence present in each of the three modified scaffolds. Moreover, we also tested the competition between the soluble peptides and the non-corresponding modified peptide scaffolds (i.e. soluble peptide YIGSR in the culture media of composite of 90% RAD16-I plus 10% TAG, etc.) as an additional control to demonstrate the specificity of each correspondent competition. As expected, the non-corresponding competitions did not change significantly the increase in cell growth observed with the corresponding soluble peptide/modified scaffold pair (Fig. 7A and B). Moreover, we tested cell viability (by Trypan blue exclusion assay) for all these experiments. We observed that the viability was very similar for all the cases (>85%) including cultures treated with soluble peptide motifs and controls (data not shown). As an example, the monolayers obtained after the competition assay with the peptide scaffold YIG shows cells covering the surface of the peptide scaffold for all cases except for the corresponding incubation with the soluble peptide YIGSR (Fig. 7C). This result suggests that the differences in cell number observed for each case were mainly due to differential cell growth rather than cell death.

### 3.5. Production of basement membrane components and NO release

To study the endothelial cell phenotype on different peptide scaffold conditions we analyzed the production of laminin 1 and collagen IV by the HAEC as a way to measure the capacity of the cells to deposit their own basement membrane components over time. In general, for all conditions tested (Fig. 8), including the RAD16-I peptide, laminin 1 and collagen IV deposition was observed when compared to conventional 2D tissue culture plates (Fig. 8A). Interestingly, only one band for laminin (B2 chain) was observed while two bands of smaller molecular weight for collagen IV were observed, suggesting that the collagen molecule may be partially degraded under the culture conditions tested, whereas the laminin molecule appears to be intact (Fig. 8A). These results may suggest that the basement membrane components deposited may be selectively undergoing remodeling, as shown by the partial degradation of the collagen IV molecule component only (Fig. 8A).

Moreover, NO release by HAEC was also estimated by assessing nitrite ( $\text{NO}_x$ ) concentrations in the cell culture supernatants. This parameter estimates the endothelial cell phenotype of the HAEC cultured on the four different peptide nanofiber scaffolds. These scaffold cultures, except for the functionalized peptide RYV, promote NO release (Fig. 8B). This result suggests that the peptide hydrogel in general is a good

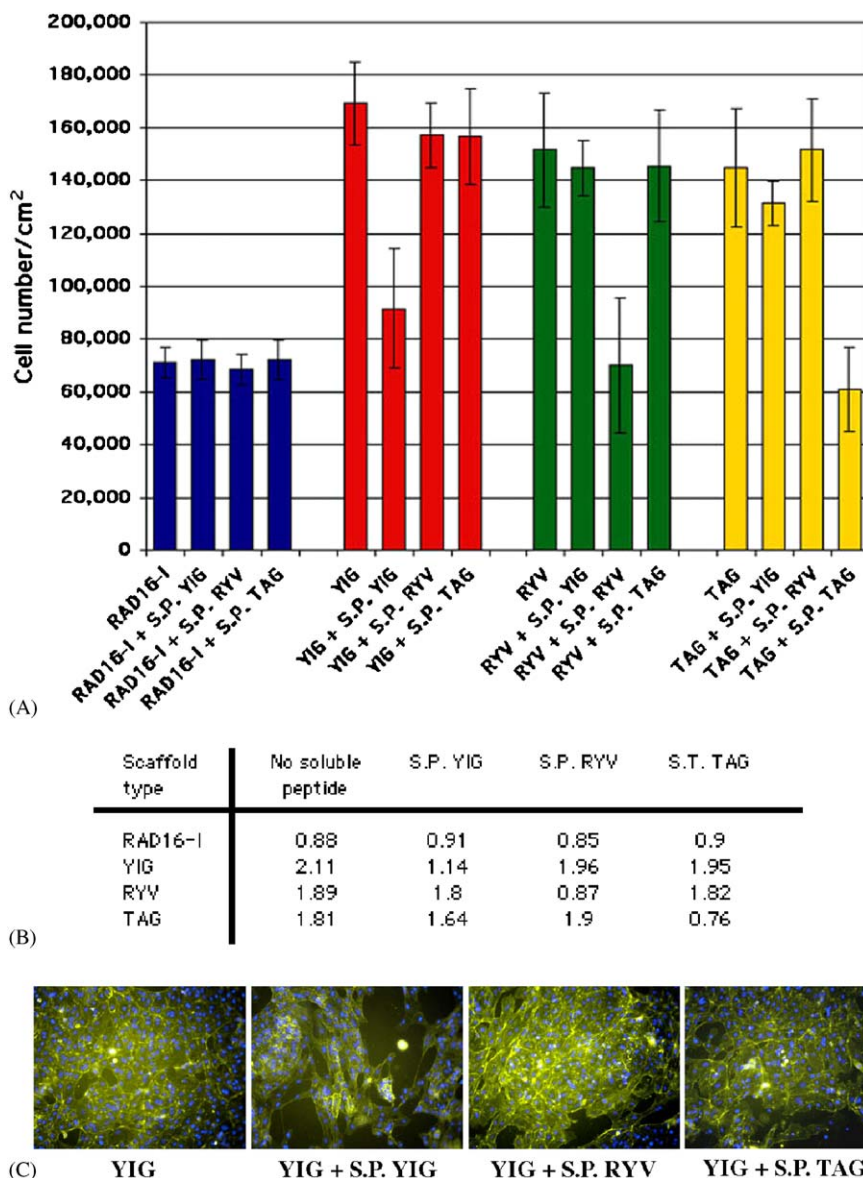


Fig. 7. Competition assay of HAEC growth with soluble peptide motifs. Cells were seeded on top of different peptide scaffold compositions ( $8 \times 10^4$  cell/cm<sup>2</sup>) and cultured for 3 days in presence or absence of soluble peptide motifs. Cell numbers were calculated for each case and expressed in number of cells per cm<sup>2</sup>. (A) RAD16-I, 100% of control peptide scaffold; RAD16-I+S.P.YIG, control peptide scaffolds with soluble peptide motif YIGSR (400  $\mu$ M); RAD16-I+S.P.RYV, control peptide scaffold with soluble peptide motif RYVVLPR (400  $\mu$ M); RAD16-I+S.P.TAG, control peptide scaffold with soluble peptide motif TAGSCLRKFSTM (400  $\mu$ M); YIG, blending 90% RAD16-I/10% YIG peptide scaffold (v/v); YIG+S.P.YIG, YIG peptide scaffolds with soluble peptide motif YIGSR (400  $\mu$ M); YIG+S.P.RYV, YIG peptide scaffold with soluble peptide motif RYVVLPR (400  $\mu$ M); YIG+S.P.TAG, YIG peptide scaffold with soluble peptide motif TAGSCLRKFSTM (400  $\mu$ M); RYV, blending 90% RAD16-I/10% RYV peptide scaffold (v/v); RYV+S.P.YIG, RYV peptide scaffolds with soluble peptide motif YIGSR (400  $\mu$ M); RYV+S.P.RYV, RYV peptide scaffold with soluble peptide motif RYVVLPR (400  $\mu$ M); RYV+S.P.TAG, RYV peptide scaffold with soluble peptide motif TAGSCLRKFSTM (400  $\mu$ M); TAG, blending 90% RAD16-I/10% TAG peptide scaffold (v/v); TAG+S.P.YIG, TAG peptide scaffolds with soluble peptide motif YIGSR (400  $\mu$ M); TAG+S.P.RYV, TAG peptide scaffold with soluble peptide motif RYVVLPR (400  $\mu$ M); TAG+S.P.TAG, TAG peptide scaffold with soluble peptide motif TAGSCLRKFSTM (400  $\mu$ M). (B) Initial seeding number ( $8 \times 10^4$  cell/cm<sup>2</sup>) was used to calculate fold changes in cell numbers after three days in culture for each of the conditions described above. (C) The competitive assay series with the scaffold YIG (blending 90% RAD16-I/10% YIG peptide scaffold, v/v) described in (A) is visualize after staining with TRITC-Phalloidin (actin fibers, yellow) and DAPI (nucleus, blue).

substrate for promoting NO release of endothelial cells. Nevertheless, there was little difference in NO release between the RAD16-I, YIG, and TAG scaffolds, it is possible that for the case of the scaffold RYV the functionalization might inhibit such activity (Fig. 8B).

#### 4. Discussion

In this work we described the development of a new biomimetic material, a functionalized self-assembling peptide scaffold, with similar properties to cellular

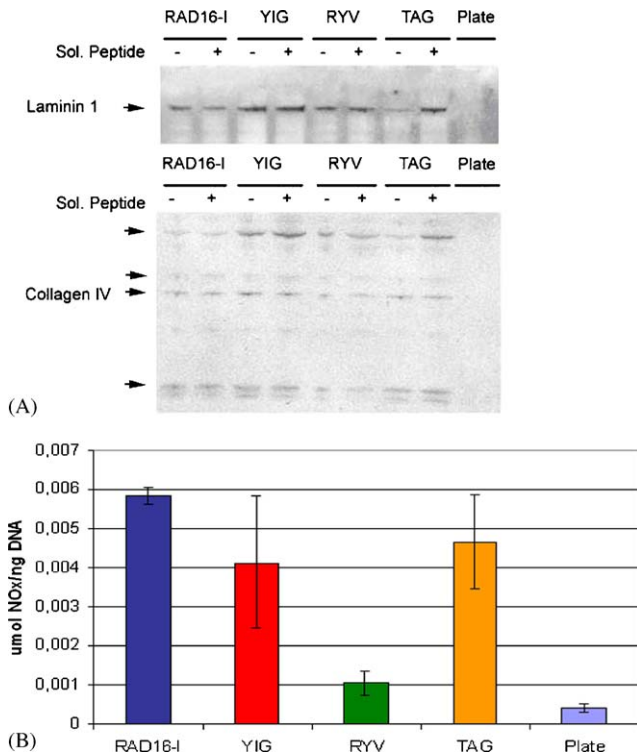


Fig. 8. (A) Western blot analysis of Laminin 1 and Collagen IV production by HAEC cultured on different peptide scaffolds and control plate (see materials and methods). (B) NO production of HAEC cultured on different peptide scaffolds and control plate (see materials and methods).

basement membrane. We selected two sequence motifs from laminin 1 (YIGSR, RYVVLPR) and one from collagen IV (TAGSCLRKFSTM) with known biological activities [3–8] to tag at the amino termini of the self-assembly sequence AcN–RADARADARA–DARADA–CONH<sub>2</sub> and obtain a functionalized self-assembling scaffold. We first studied the structural properties of the functionalized peptides to determine their solubility and capacity to form hydrogels. In view of the extensions added to the self-assembling peptide (between 5 and 12 extra residues) we expected to see changes in the  $\beta$ -sheet structure (CD), fiber formation (AFM) as well as their viscoelastic properties (rheometry). In fact, those parameters were affected in the functionalized peptides resulting in hydrogels with weaker  $\beta$ -sheet structure, as shown by a decrease in the intensity of mole residue ellipticity at 216 nm (Fig. 2) and, as a consequence, a change in the viscoelastic properties. For instance, the storage modulus  $G'$  in the hydrogel RAD16-I reaches  $2.5 \times 10^3$  Pa, is greater than the loss modulus  $G''$  and, both remain relatively constant with oscillatory frequency (Fig. 4). The magnitude of  $G'$  is 100 times lower for the functionalized peptides YIG and RYV and 1000 times lower for the peptide TAG. They are still greater than their respective loss modulus  $G''$  and again, both remain relatively

constant with oscillatory frequency, indicating they have gel-like property (Fig. 4). These results indicate that the addition of the additional motif interferes with the self-assembling process due to the possible distortion of the  $\beta$ -sheet configuration, producing softer hydrogels.

In order to obtain hydrogels with comparables viscoelastic properties we decided to blend the functionalized peptides with the self-assembling peptide RAD16-I in a 1:9 ratio. In this way we generated three hydrogel mixes, named YIG, RYV and TAG, with similar mechanical properties to the unmodified RAD16-I scaffold. The four surfaces were tested for HAEC attachment, growth, and endothelial cell phenotype.

We observed that cell attachment for all the surfaces tested was close to 100% suggesting that the modifications are not playing an important role under the culture conditions tested (not shown). Interestingly, the functionalized peptide scaffolds promoted maintenance and growth of HAEC over time in culture. In particular, sub-confluent seeded cultures of HAEC developed into confluent monolayers with elevated number of cells when compared with the non-functionalized scaffold, suggesting their role in increasing growth rates (Figs. 6 and 7). In addition, growth rates in the non-functionalized RAD16-I scaffold did not change over time, suggesting that cells under these conditions remain mainly inactive, probably they do not spread or migrate well and, as a consequence, they do not proliferate (Figs. 6 and 7). Most importantly, competition assays with each corresponding soluble motif designed to block specific interactions between cells and the functionalized scaffolds demonstrated that growth rates were reduced to levels similar to control RAD16-I scaffold, suggesting that the cells indeed recognized the exposed adhesion motifs attached to each scaffold (Fig. 7). Therefore, it appears that endothelial cell growth was modulated through the biomimetic surface matrix only when the sequence was physically attached to the nanofiber (Fig. 1B), and that specific interaction in each case can be disrupted by adding the same soluble non-attached peptide motif. It is plausible that in this case a mechano-signaling transduction event that regulates the cell growth and monolayer formation of HAEC was involved. This is of critical importance for endothelial cells during neovascularization of multiple physiological and pathological processes, including wound healing, menstrual regeneration of endometrium, tumor angiogenesis, etc [36–38]. These results are consistent with a previous report describing that immobilized YIGSR peptide on the synthetic polymers, PET or PTFE, promoted endothelial cell adhesion and cell spreading [28].

Moreover, the peptide scaffolds in general enhanced the endothelial cell phenotype, such as NO synthesis and deposition of basement membrane components (laminin

I and collagen IV). This suggests that HAEC cultured under these peptide scaffold conditions perform better in terms of recreating the endothelial microenvironment.

## 5. Conclusions

We have developed a new class of biomimetic material, tailor-made peptide scaffolds, with potential signaling capacity to enhance endothelial cell phenotype. The use of these functionalized scaffolds can be expanded to the study of cell receptor–matrix interactions in a more detailed way. For instance, the use of the functionalized peptide scaffold carrying the motif YIGSR—a minimum recognition sequence for the 67 kDa laminin receptor (67LR) [17]—will be crucial for the study the cell receptor–matrix process in a more controlled system. These studies can be use in specific areas such as the involvement of the 67LR in shear stress-dependent responses in endothelial cells [39], early stages in the development of tumor formation and metastatic phenotype [40], as well as YIGSR-mediated cell spreading in a variety of cell types [41]. These examples illustrate the diverse possibilities of studies that can be conducted with the functionalized scaffolds and suggest that the biomimetic material can be used to recognize new potential extracellular matrix recognition domains in components not only present in the basement membrane but also in the matrix of cellular events such as wound healing and tissue regeneration. We conclude that tailor-made peptide scaffolds represent a new generation of cell-responsive materials, easy to synthesize and scale-up, and likely to have an impact on diverse areas of biomedical research, biotechnology, and regenerative biology.

## Acknowledgements

We gratefully acknowledge Hidenori Yokoi, Andrea Lomander and Geoff Becker for their technical help and advice in some aspects of the work. We specially thank Wonmuk Hwang for the peptide nanofiber molecular model and Angelo Cardoso, Roger Kamm and Alisha Sieminski for helpful discussions. This work was supported primarily by the Engineering Research Centers Program of the National Science Foundation under NSF Award Number 9843342.

## References

[1] Zhang S, Holmes T, Lockshin C, Rich A. Spontaneous assembly of a self-complementary oligopeptide to form a stable macroscopic membrane. *Proc Natl Acad Sci USA* 1993;90:3334–8.

[2] Zhang S, Holmes T, DiPersio M, Hynes RO, Su X, Rich A. Self-complementary oligopeptide matrices support mammalian cell attachment. *Biomaterials* 1995;16:1385–93.

[3] Skubitz AP, McCarthy JB, Zhao Q, Yi XY, Furcht LT. Definition of a sequence, RYVVLPR, within laminin peptide F-9 that mediates metastatic fibrosarcoma cell adhesion and spreading. *Cancer Res* 1990;50:7612–22.

[4] Sakamoto N, Iwahana M, Tanaka NG, Osada Y. Inhibition of angiogenesis and tumor growth by a synthetic laminin peptide, GDPGYIGSR-NH<sub>2</sub>. *Cancer Res* 1991;51:903–6.

[5] Iwamoto Y, Robey FA, Graf J, Sasaki M, Kleinman HK, Yamada Y, Martin GR. YIGSR, a synthetic laminin pentapeptide, inhibits experimental metastasis formation. *Science* 1987;238:1132–4.

[6] Kleinman HK, Graf J, Iwamoto Y, Sasaki M, Schasteen CS. Identification of a second active site in laminin for promotion of cell adhesion and migration and inhibition of melanoma lung colonization. *Arch Biochem Biophys* 1989;272:39–45.

[7] Koliakos GG, Koliakos KK, Furcht LT, Reger LA, Tsilibary EC. The binding of heparin to the type IV collagen: domain specificity with identification of peptide sequences from the alpha 1 (IV) and alpha 2 (IV) which preferentially bind heparin. *J Biol Chem* 1989;264:2313–23.

[8] Tsilibary EC, Reger LA, Vogel AM, Koliakos GG, Anderson SS, Charonis AS, Alegre JN, Furcht LT. Identification of a multifunctional, cell-binding peptide sequence from the  $\alpha$ 1(NC1) of type IV collagen. *J Cell Biol* 1990;111:1583–91.

[9] Beck H, Hunter I, Engel J. Structure and function of laminin: anatomy of a multidomain glycoprotein. *FASEB J* 1990;4:148–60.

[10] Engel J. Laminins and other strange proteins. *Biochemistry* 1992;31:10643–51.

[11] Kreis T, Vale R. editors. *Guidebook of the extracellular, anchor and adhesion proteins*. Second ed. UK: A Sabrook & Tooze publication at Oxford University Press; 1999.

[12] Yurchenco PD, O'Rear JJ. Basement membrane assembly. *Methods Enzymol* 1994;145:489–518.

[13] Grant DS, Tashirom KI, Segui-Real B, Yamada Y, Martin GR, Kleinman HK. Two different laminin domains mediate the differentiation of human endothelial cells into capillary-like structures in vitro. *Cell* 1989;58:933–43.

[14] Ponce ML, Nomizu M, Delgado MC, Kuratomi Y, Hoffman MP, Powell S, Yamada Y, Kleinman HK, Malinda KM. Identification of endothelial cell binding sites on the laminin  $\gamma$ 1 chain. *Circ Res* 1999;84:688–94.

[15] Malinda KM, Nomizu M, Chung M, Delgado M, Kuratomi Y, Yamada Y, Kleinman HK, Ponce ML. Identification of laminin  $\alpha$ 1 and  $\beta$ 1 chain peptides active for endothelial cell adhesion, tube formation and aortic sprouting. *FASEB J* 1999;13:53–62.

[16] Kubota Y, Kleinman HK, Martin GR, Lawley TJ. Role of laminin and basement membrane in the morphological differentiation of human endothelial cells into capillary-like structures. *J Cell Biol* 1988;107:1589–98.

[17] Graf J, Ogle RC, Robey FA, Sasaki M, Martin GR, Yamada Y, Kleinman HKA. A pentapeptide from the laminin  $\beta$ 1 chain mediates cell adhesion and binds the 67000 laminin receptor. *Biochemistry* 1987;26:6896–900.

[18] Davis GE, Black SM, Bayless KJ. Capillary morphogenesis during human endothelial cell invasion of three-dimensional collagen matrices. *In Vitro Cell Dev Biol Animal* 2000;36:513–9.

[19] Davis GE, Bayless KJ, Mavila A. Molecular basis of endothelial cell morphogenesis in three-dimensional extracellular matrices. *Anat Rec* 2002;268:252–75.

[20] Bell SE, Mavila A, Salazar R, Bayless KJ, Kanagala S, Maxwell SA, Davis GE. Differential gene expression during capillary morphogenesis in 3D collagen matrices: regulated expression of genes involved in basement membrane matrix assembly, cell cycle

- progression, cellular differentiation and G-protein signalling. *J Cell Science* 2001;114:2755–73.
- [21] Charonis AS, Tsilibary EC, Yurchenco PD, Furthmayr H. Binding of laminin to type IV collagen: a morphological study. *J Cell Biol* 1985;100:1848–53.
- [22] Paulsson M, Aumailley M, Deutzmann R, Timpl R, Beck K, Engel J. Laminin-nidogen complex. Extraction with chelating agents and structural characterization. *Eur J Biochem* 1987;166:11–9.
- [23] Poschl E, Mayer U, Stetefeld J, Baumgartner R, Holak TA, Huber R, Timpl R. Site-directed mutagenesis and structural interpretation of the nidogen-binding site of the laminin  $\gamma$ 1 chain. *EMBO J* 1996;15:5154–9.
- [24] Holmes TC, De Lacalle S, Su X, Liu G, Rich A, Zhang S. Extensive neurite outgrowth and active synapse formation on self-assembling peptide scaffolds. *Proc Natl Acad Sci USA* 2000;97:6728–33.
- [25] Kisiday J, Jin M, Kurz B, Hung H, Semino C, Zhang S, Grodzinsky AJ. Self-assembling peptide hydrogel fosters chondrocyte extracellular matrix production and cell division: implications for cartilage tissue repair. *Proc Natl Acad Sci USA* 2002;99:9996–10001.
- [26] Semino CE, Merok JR, Crane G, Panagiotakos G, Zhang S. Functional differentiation of hepatocyte-like spheroid structures from putative liver progenitor cells in three-dimensional peptide scaffolds. *Differentiation* 2003;71:262–70.
- [27] Semino CE, Kasahara J, Hayashi Y, Zhang S. Entrapment of migrating hippocampal neural cells in 3-D peptide nanofiber scaffold. *Tissue Eng* 2004;10:643–55.
- [28] Massia SP, Hubbell JA. Human endothelial cell interactions with surface-coupled adhesion peptides on non-adhesive glass and two polymeric biomaterials. *J Biomed Mater Res* 1991;2: 223–42.
- [29] Lin HB, Sun W, Mosher DF, Garcia-Echeverria C, Schaufelberger K, Lelkes PI, Cooper SL. Synthesis, surface, and cell-adhesion properties of polyurethanes containing covalently grafted RGD-peptides. *J Biomed Mater Res* 1994;3:329–42.
- [30] Schmedlen RH, Masters KS, West JL. Photocrosslinkable polyvinyl alcohol hydrogels that can be modified with cell adhesion peptides for use in tissue engineering. *Biomaterials* 2002;23:4325–32.
- [31] Sagnella SM, Kligman F, Anderson EH, King JE, Murugesan G, Marchant RE, Kottke-Marchant K. Human microvascular endothelial cell growth and migration on biomimetic surfactant polymers. *Biomaterials* 2004;25:1249–59.
- [32] Hartgerink JD, Beniash E, Stupp SI. Self-assembly and mineralization of peptide-amphiphile nanofibers. *Science* 2001;294: 1684–8.
- [33] Silva GA, Czeisler C, Niece KL, Harrington D, Kessler J, Stupp SI. Selective differentiation of neuronal progenitor cells by high-epitope density nanofibers. *Science express*; 2004.
- [34] Brooks BR, Bruccoleri RE, Olafson BD, States DJ, Swaminathan S, Karplus M. CHARMM: a program for macromolecular energy, minimization, and dynamics calculations. *J Comp Chem* 1983;4:187–217.
- [35] Humphrey W, Dalke A, Schulten K. VMD—Visual Molecular Dynamics. *J Molec Graphics* 1996;14:33–8.
- [36] Reed MJ, Sage EH. SPARC and the extracellular matrix: implications for cancer and wound repair. *Curr Top Microbiol Immunol* 1996;213:81–94.
- [37] Ferenczy A, Bertrand G, Gelfand MM. Proliferation kinetics of human endometrium during the normal menstrual cycle. *Am J Obstet Gynecol* 1979;133:859–67.
- [38] Bogenrieder T, Herlyn M. Axis of evil: molecular mechanism of cancer metastasis. *Oncogene* 2003;22:6524–36.
- [39] Gloe T, Riedmayrs S, Sohn H-Y, Pohl U. The 67-kDa laminin-binding protein is involved in shear stress-dependent endothelial nitric-oxide synthase expression. *J Biol Chem* 1999;274: 15996–6002.
- [40] Ardini E, Sporchia B, Pollegioni L, Modugno M, Ghirelli C, Castiglioni F, Tagliabue E, Ménard S. Identification of a novel function for 67-kDa laminin receptor: increase in laminin degradation rate and release of motility fragments. *Cancer Res* 2002;62:1321–5.
- [41] Massia SP, Rao SS, Hubbell JA. Covalently immobilized laminin peptide Tyr-Ile-Gly Ser-Arg (YIGSR) supports cell spreading and co-localization of the 67-kilodalton laminin receptor with  $\alpha$ -actinin and vinculin. *J Biol Chem* 1993;268:8053–9.